Effect of Ni loading and calcination temperature on catalyst performance and catalyst deactivation of Ni/SiO_2 in the hydrodechlorination of 1,2-dichloropropane into propylene

Young Heon Choi and Wha Young Lee *

Division of Chemical Engineering, Seoul National University, Shinlim-dong, Kwanak-ku, Seoul 151-742, Korea
E-mail: wyl@snu.ac.kr

Received 18 January 2000; accepted 19 May 2000

The hydrodechlorination of 1,2-dichloropropane (DCPA), a chlorinated organic waste which is produced in the epichlorohydrin process, to propylene was carried out over Ni/SiO_2 catalysts. The effects of Ni loading and calcination temperature on catalyst performance and catalyst deactivation of Ni/SiO_2 were systematically investigated. The Ni/SiO_2 catalysts efficiently converted DCPA into propylene in 95% selectivity or higher. The particle size of Ni on SiO_2 was strongly related to the catalyst stability. In terms of the effect of Ni loading, the largest Ni particles on SiO_2 showed the best durability against deactivation. A series of TPR and UV-DRS measurements revealed that nickel hydrosilicate was formed as the result of the interaction between Ni and SiO_2. Nickel hydrosilicate was found to be responsible for the catalyst stability leading to low catalyst deactivation. HCl adsorption on Ni/SiO_2 was the main reason for catalyst deactivation. HCl modified the crystal structure of metallic Ni to $NiCl_2$ and led to irreversible deactivation and metal sintering.

Keywords: Ni/SiO_2, hydrodechlorination, 1,2-dichloropropane, nickel hydrosilicate, particle size, deactivation, HCl, nickel–chlorine interaction, metal sintering

1. Introduction

The treatment of chlorinated industrial organic waste which was generated in the form of chlorinated alkanes, alkenes and aromatic compounds is a very important issue in the environmental sense, because most of these waste materials are thermally unstable and very toxic. Considerable efforts have been made to eliminate such compounds from waste streams. Several approaches for reducing or eliminating chlorinated organic waste include direct incineration [1], catalytic combustion [2], biodegradation [3], photo-catalytic decomposition [4] and catalytic hydrodechlorination [5]. Among these methods, the catalytic conversion of chlorinated organic waste into useful hydrocarbons via hydrodechlorination represents one of the more promising methods, since toxic compounds such as Cl_2, $COCl_2$, and fragments of the parent chlorocarbons are not formed in the hydrodechlorination processes. In addition to environmental advantages, this process has clear economic merits because the resulting hydrocarbons can be recovered and recycled. Therefore, the catalytic conversion of chlorinated hydrocarbons into alkanes by hydrogenolysis represents a subject of considerable interest [6].

The catalytic systems studied in hydrogenolysis can be classified into two groups. The first group involves the use of metals such as Pd, Pt or Rh supported on γ-Al_2O_3, SiO_2 or active carbons. Scott et al. [7] examined the activity of a Pd/ZnO catalyst supported on γ-Al_2O_3 in the hydrogenolysis of 1,1,2-trichlorotrifluoroethane and found that the activity loss during the hydrogenolysis was due to the formation of nonlabile halogen at the metal function. Coq et al. [8] also investigated the effects of hydrogen on the hydrodechlorination of dichlorofluoromethane over supported Pd catalysts. In the hydrodechlorination of 1,2-dichloroethane into ethylene over Pd–Ag catalysts, the addition of silver enhanced the selectivity for ethylene [9]. Harley et al. [10] also reported on the hydrodechlorination of 1,2-dichloropropane into propylene over Pt/Cu/C catalysts. He claimed that the second metal, Cu, promoted activity due to the surface segregation effect of the added Cu. A major advantage of these noble metal catalysts is their superior activity and selectivity, even at low temperatures and pressures. However, single noble metal catalysts, such as Pt/Al_2O_3, Pd/Al_2O_3 and Rh/Al_2O_3 have the disadvantage of being susceptible to rapid deactivation [11,12]. Therefore, the studies on the addition of a second metal into such noble metal catalysts have been intensively investigated [9,13].

The second group catalysts are hydrotreating catalysts such as Ni–Mo/γ-Al_2O_3 or Co–Mo/γ-Al_2O_3. However, these catalysts require high temperatures and pressures in order to achieve a reasonable level of catalytic activity.

Recently, new studies have been carried out relative to the conversion of chlorinated hydrocarbons into more useful unsaturated hydrocarbons. Some groups, who studied supported noble metal catalysts [9,13], claimed that the formation of the unsaturated hydrocarbons was con-

* To whom correspondence should be addressed.

siderably affected by the added second metal as a promoter.

Some studies have also been carried out with the Ni-loaded catalysts for the selective hydrodechlorination of chlorinated hydrocarbons into alkenes [14]. Mori et al. [15] reported that a 95% selectivity could be achieved with a Ni/SiO_2 catalyst in the hydrodechlorination of CCl_2FCClF_2 to $CClF{=}CF_2$. However, the mechanism of formation of unsaturated hydrocarbon by Ni supported catalysts has not been clearly elucidated.

In this study, the catalytic hydrodechlorination of 1,2-dichloropropane, a major by-product of the epichlorohydrin process, into propylene was carried out over Ni/SiO_2 catalysts in a continuous-flow fixed-bed reactor. The effects of the amount of Ni loading and the calcination temperature on the catalyst performance and catalyst deactivation were intensively investigated. In order to define the effect of HCl on the catalyst deactivation, the hydrogenation of propylene over Ni/SiO_2 catalysts was also examined. Various supports were also examined for the hydrodechlorination, in order to elucidate the deactivation of the Ni catalyst. Ni/SiO_2 catalysts were characterized by H_2 chemisorption, XRD, TPR, UV-DRS, TEM and elemental analysis.

2. Experimental

2.1. Catalyst preparation

Ni/SiO_2 catalysts were prepared by the incipient wetness impregnation of SiO_2 (JRC-SIO-7, surface area = 157 m^2/g, pore volume = 1.5 ml/g) with appropriate amounts of aqueous solution of nickel nitrate ($Ni(NO_3)_2{\cdot}6H_2O$). After drying overnight at 373 K, the catalysts were calcined for 5 h at various temperatures under a stream of air. The Ni/SiO_2 catalysts prepared with various levels of Ni loading and at variety of calcination temperatures were denoted as $x\mathrm{Ni}/\mathrm{SiO}_2(y)$, where x represents the wt% of Ni loading and y the calcination temperature (K). For example, $10\mathrm{Ni}/\mathrm{SiO}_2(723)$ indicates that Ni loading on SiO_2 was 10 wt% and the catalyst was calcined at 723 K.

2.2. Catalyst characterization

Catalysts were characterized by H_2 chemisorption, TPR (temperature-programmed reduction), UV-DRS (ultraviolet diffuse reflectance spectroscopy), XRD (X-ray diffraction), TEM (transmission electron microscopy) and elemental analysis.

The chemisorption of hydrogen was measured in a chemisorption unit. A 0.2 g catalyst sample was placed in a glass U-tube sample holder, reduced under hydrogen flow at 673 K for 2 h. After the reduction, the sample was evacuated for 1 h at the temperature of reduction, and cooled under vacuum (1×10^{-4} Torr) to the measurement temperature, 293 K, and isotherms for total and irreversible adsorption were determined.

The TPR measurement was carried out in a conventional flow system with moisture trap connected to a TCD at temperatures ranging from room temperature to 1073 K with a heating rate of 5 K/min. The flow rate of the reducing gas was $H_2 = 6$ ml/min and $N_2 = 34$ ml/min for 0.1 g of catalyst.

The symmetry and crystallinity of the Ni/SiO_2 catalysts were confirmed by XRD (Rigaku, D/MAX-IIA).

The particle size and location of Ni on the catalyst surface were confirmed by TEM (Jeol, JXA-8900R) using an ultrasonically dispersed catalyst sample (in ethanol) deposited over a thin gold film. The Ni particle size distribution (PSD) was obtained by measuring at least ca. 200–250 particles for each catalyst sample, while the average Ni particle size (d_s) was calculated by the following normal statistical formula:

$$d_s = \frac{\sum_i n_i d_i^3}{\sum_i n_i d_i^2}.$$

The amount of coke deposition on the catalysts during the reaction was determined by elemental analysis.

The metallic states of the Ni species were confirmed by UV-DRS (Perkin–Elmer, Ramda-20 spectrometer) in the range of 200–800 nm.

2.3. Hydrodechlorination

The hydrodechlorination of 1,2-dichloropropane (DCPA) into propylene was carried out in a continuous-flow fixed-bed reactor at atmospheric pressure. The Ni/SiO_2 catalyst (200 mg) was charged in a tubular quartz reactor and activated in a stream of hydrogen (20 ml/min) and nitrogen carrier (20 ml/min) at 673 K for 2 h. DCPA (5.13×10^{-3} mol/h) and hydrogen were then fed into the reactor together with the nitrogen carrier (5.13×10^{-2} mol/h) for the reaction. The feed ratio of H_2/DCPA was varied by changing the feed rate of hydrogen. The reaction temperature was maintained at 573 K. The products were analyzed with FID in GC (HP 5890 II). Porapak Q was used as a column material.

3. Results and discussion

3.1. Temperature-programmed reduction

TPR measurements were carried out, in order to determine the behavior of nickel metal in the reduction reactions and to investigate the metal–support interactions. Table 1 shows the reduction temperature and relative reduction peak areas of NiO and nickel hydrosilicate for each catalyst. Two broad peaks were observed between 600 and 900 K at all the profiles. The peaks between 600 and 700 K represent the typical peaks for the reduced NiO species supported on SiO_2, and the peaks appearing at higher temperatures are tentatively assigned to those for a nickel hydrosilicate [16]. This suggests that a metal–support interaction exists between nickel and SiO_2. The amount of H_2 consumption

Table 1
Relative areas of TPR profiles.

Catalyst	T_1[a] (K)	A_1[b] (a.u.)	T_2[c] (K)	A_2[d] (a.u.)
5Ni/SiO_2(723)	638	60.3	725	37.07
10Ni/SiO_2(723)	641	107.1	718	42.4
10Ni/SiO_2(873)	638	133.1	750	63.6
10Ni/SiO_2(1073)	646	92.3	737	58.7
20Ni/SiO_2(723)	661	332.6	747	113
40Ni/SiO_2(723)	643	519.6	748	58.5

[a] Reduction temperature of NiO.
[b] Area of NiO reduction profile.
[c] Reduction temperature of nickel hydrosilicate.
[d] Area of nickel hydrosilicate reduction profile.

required for the reduction of NiO and nickel hydrosilicate increased with Ni loading. Two broad peaks were also observed between 600 and 900 K in the TPR profiles of the Ni/SiO_2 catalysts with respect to the calcination temperature. The highest amount of H_2 consumption for the reduction of nickel hydrosilicate was observed at a calcination temperature of 873 K, suggesting that the formation of nickel hydrosilicate is strongly related to the calcination temperature. The 20Ni/SiO_2(723) catalyst showed the maximum value of reduction peak area of nickel hydrosilicate.

3.2. UV-DRS analysis

In order to confirm the identity of the nickel species and the formation of nickel hydrosilicate, UV-DRS for Ni/SiO_2 catalysts was measured. Figure 1 shows the UV-DRS profiles for the Ni/SiO_2 catalysts in the visible range with respect to the amount of nickel loading. All catalysts showed two distinctive major bands at 430 nm and in the range of 710–730 nm and a minor band at 550 nm. According to a previous report [17] on UV-DRS measurements of a nickel oxide catalyst supported on alumina, the band at 430 nm represents the octahedrally coordinated Ni^{2+} species and the band in the range of 710–730 nm represents the tetrahedrally coordinated Ni^{2+} species. The authors of [17] also reported that a band appeared in the range 590–630 nm, which corresponded to the nickel spinel species. Therefore, it is concluded that the two major bands in figure 1 correspond to the octahedrally coordinated and the tetrahedrally coordinated Ni^{2+} species. Although no UV-DRS peak was observed at ranges from 590 to 630 nm in the Ni/SiO_2 catalyst, it is inferred that the band at 550 nm might be due to the nickel spinel species. As the nickel loading increased, the amounts of tetrahedrally coordinated Ni^{2+} species also increased. From this result, we can conclude that the tetrahedrally coordinated Ni^{2+} can be attributed to the formation of nickel hydrosilicate.

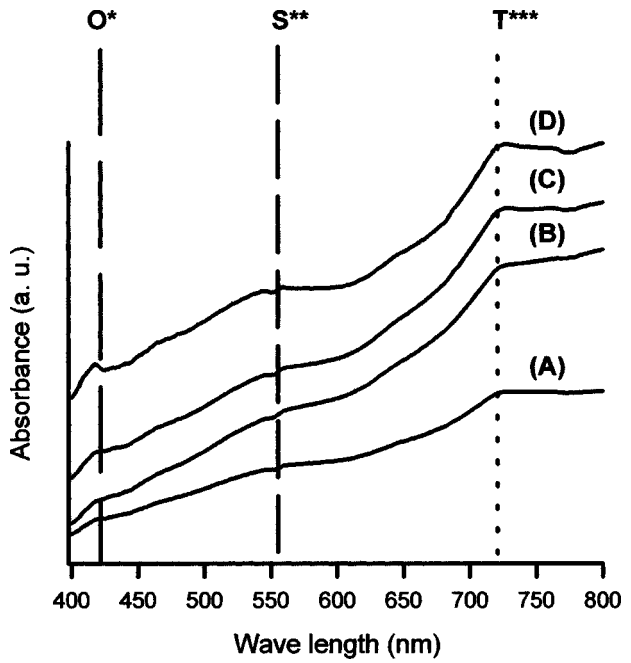

Figure 1. UV-DRS profiles of Ni/SiO_2 catalysts as a function of Ni loading (O* – octahedrally coordinated Ni^{2+}, S** – nickel spinel species, T*** – tetrahedrally coordinated Ni^{2+}): (A) 5Ni/SiO_2(723), (B) 10Ni/SiO_2(723), (C) 20Ni/SiO_2(723) and (D) 40Ni/SiO_2(723).

3.3. Hydrodechlorination of 1,2-dichloropropane (DCPA)

Figure 2 shows the typical catalytic activity of the 10Ni/SiO_2(723) catalyst for the vapor phase hydrodechlorination of 1,2-dichloropropane (DCPA) at 573 K. The main product was propylene. The selectivity for propylene was 95% or higher. Small amounts of 1-chloropropylene and 3-chloropropylene were formed in the reaction, and trace amounts of methane, ethane and ethylene were also detected. The conversion was decreased by ca. 35% after 20 h of time-on-stream and thereafter remained constant.

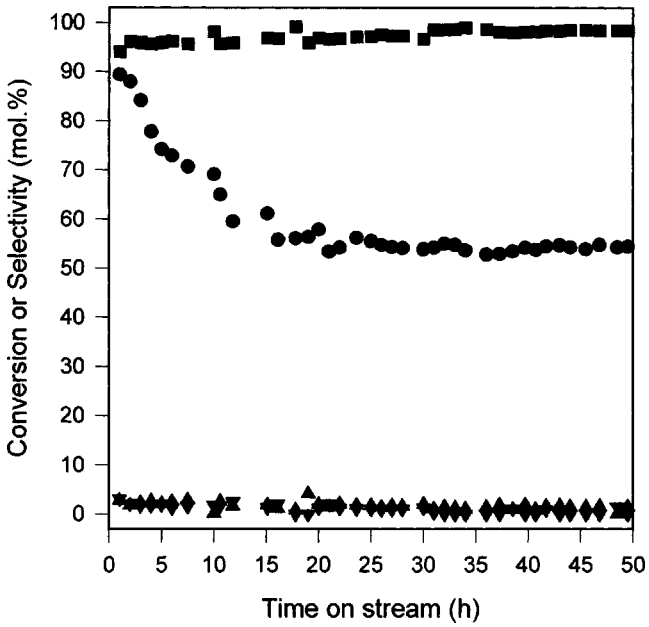

Figure 2. Catalytic activity and product distribution of the 10Ni/SiO_2(723) catalyst with respect to time-on-stream; reaction temperature 573 K, H_2/DCPA = 10. (●) Conversion, (■) propylene, (▲) 1-chloropropylene, (▼) 3-chloropropylene.

Table 2
Catalytic performance of 10Ni/SiO_2(723) with respect to the hydrodechlorination of DCPA with respect to the mole ratio of H_2/DCPA feed at 573 K after a 10 h run.

H_2/DCPA	Conversion (%)	Product selectivity (mol%)		
		Propylene	1-chloropropylene	3-chloropropylene
0	8.92	16.12	40.90	42.98
1	15.40	85.58	0.06	14.36
3	37.16	96.84	0.06	3.10
6	67.24	97.17	0.05	2.78
10	69.14	98.15	0.02	1.83
20	77.94	95.78	0.02	4.20

The product selectivities remained nearly constant with the time-on-stream.

The performance of the 10Ni/SiO_2(723) catalyst for the hydrodechlorination of DCPA with respect to the feed mole ratio of H_2/DCPA at 573 K after a 10 h run is summarized in table 2. In the absence of hydrogen in the feed, DCPA is mainly converted into 1- and 3-chloropropylene. However, the propylene selectivity increased rapidly with an increase in the mole ratio of H_2/DCPA. When the mole ratio exceeded 6, no significant changes were observed in the conversion and the product distribution. This can be explained by the competitive adsorption of hydrogen and HCl on the catalyst surface [18]. An increase of H_2 partial pressure may inhibit the adsorption of HCl on the metal and hydrogen plays a role in the cleaning of the metal surface [12]. It is also noteworthy that propane was not produced even for the case of a high feed mole ratio of H_2/DCPA. There are two possible explanations for these phenomena. One is that, since the activation energy required for the hydrogenation of a double bond in the unsaturated hydrocarbons is higher than that for the cleavage of a C–Cl bond [8], the dechlorination reaction might be faster than the further hydrogenation of propylene to propane in the hydrodechlorination of DCPA. The other possible explanation is that HCl, which is adsorbed on the catalyst surface, could inhibit the ability of nickel to catalyze the hydrogenation reaction [18].

In order to identify the crystal structure of Ni and to confirm the formation of HCl during the hydrodechlorination of DCPA, XRD measurements were performed for the freshly reduced and used catalysts. Figure 3 shows the XRD patterns of the freshly reduced Ni/SiO_2 catalysts with respect to Ni loading. Three major XRD peaks were observed for all catalysts, and the XRD patterns of all Ni/SiO_2 catalysts were all identical. The characteristic three peaks at 44.4°, 51.7° and 76.3° clearly indicate that the metallic nickel has a cubic symmetry. However, the XRD patterns of the used Ni/SiO_2 catalysts were different from those of the freshly reduced Ni/SiO_2 catalysts, as shown in figure 4. The peaks at 39.2°, 41.5° and 44.5° are characteristic peaks of the hexagonal symmetry of nickel. This suggests that some of the nickel cubic structure was converted to a hexagonal symmetry during the reaction. In addition, the characteristic peak of $NiCl_2$ at 15.2° ($NiCl_2$ [003]) was observed in case of the used Ni/SiO_2 catalysts. These results clearly indicate that HCl was formed during the hydrodechlorination and that HCl altered the crystal structure of metallic nickel. Choi et al. [19] reported that for the hydrodechlorination of carbon tetrachloride over Pt/MgO, a basic support, MgO was converted to $MgCl_2$. In the reaction conditions employed here, however, no evidence for the interaction between HCl and SiO_2 was detected.

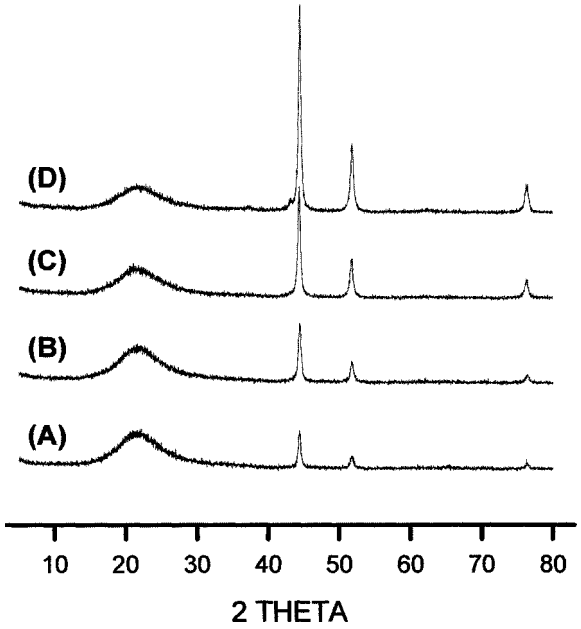

Figure 3. XRD patterns of freshly reduced Ni/SiO_2 catalysts as a function of Ni loading: (A) 5Ni/SiO_2(723), (B) 10Ni/SiO_2(723), (C) 20Ni/SiO_2(723) and (D) 40Ni/SiO_2(723).

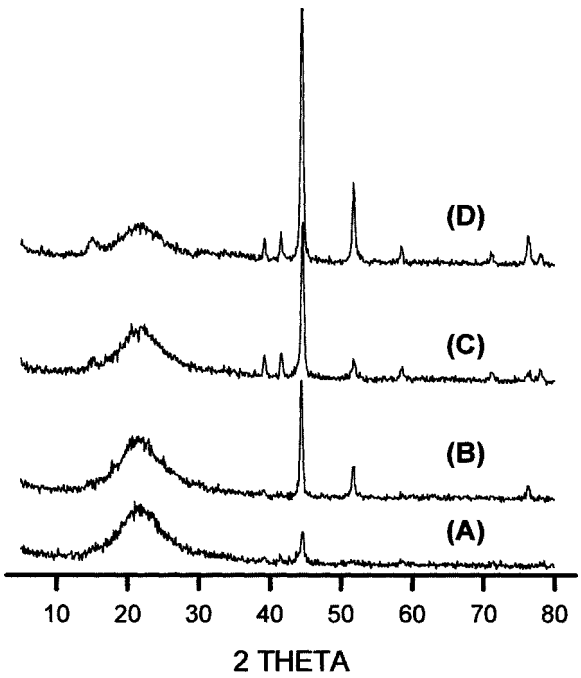

Figure 4. XRD patterns of used Ni/SiO_2 catalysts for 10 h of hydrodechlorination with respect to Ni loading: (A) 5Ni/SiO_2(723), (B) 10Ni/SiO_2(723), (C) 20Ni/SiO_2(723) and (D) 40Ni/SiO_2(723).

Table 3 shows the catalytic performance of Ni/SiO_2 with respect to Ni loading at 573 K after a 10 h run.

Table 3
Catalytic performance of Ni/SiO_2 with respect to the hydrodechlorination of DCPA as a function of Ni loading at 573 K after a 10 h run (H_2/DCPA = 10).

Catalyst	TOF (s^{-1}) $\times 10^2$		Deactivation	Product selectivity (mol%) at 10 h		
	1 h	10 h	(%)	Propylene	1-chloropropylene	3-chloropropylene
$5Ni/SiO_2(723)$	2.07	1.30	37.40	97.25	2.57	0
$10Ni/SiO_2(723)$	4.49	3.49	22.31	98.15	0.02	1.83
$20Ni/SiO_2(723)$	2.14	1.95	9.14	98.41	1.23	0.07
$40Ni/SiO_2(723)$	2.24	1.97	12.05	98.31	1.45	0.04

Table 4
Characteristics of Ni/SiO_2 catalysts.

Catalyst	Dispersion	Nickel particle size by TEM (nm)	
	(%)	Reduced	Used
$5Ni/SiO_2(723)$	37.07	25.2	30.5
$10Ni/SiO_2(723)$	9.06	34.8	50.7
$20Ni/SiO_2(723)$	10.69	50.6	60.6
$40Ni/SiO_2(723)$	6.89	46.3	51.9

10% Ni/SiO_2 showed the maximum TOF for the DCPA hydrodechlorination reaction. However, its deactivation rate was rather high. The $20Ni/SiO_2(723)$ catalyst showed the best stability with respect to deactivation. This result can be explained by two facts. One is the Ni particle size. In order to examine the catalytic performance with respect to particle size, TEM was used to measure the particle sizes of various Ni catalysts and these results are shown in table 4. It was found that the particle size of the used catalysts was larger than that of the fresh catalysts for all catalysts. This suggests that the particle size of the metal is increased due to metal sintering which may be caused by HCl during the reaction. Tables 3 and 4 showed the good correlation between the deactivation rate and Ni particle sizes. The bigger the Ni particle size, the lower was the deactivation.

The other one is the amount of nickel hydrosilicate. From the results of TPR of Ni/SiO_2 catalysts in table 1 and the catalytic performance in table 3, it was revealed that catalyst deactivation decreased with the increment of nickel hydrosilicate. The influence of nickel hydrosilicate was also investigated with variation in the calcination temperature of catalysts. The effect of calcination temperature on the catalytic activity at 573 K is shown in figure 5. The $10Ni/SiO_2(723)$ and $10Ni/SiO_2(1073)$ catalysts showed a severe deactivation. However, the $10Ni/SiO_2(873)$ catalyst showed a stable catalytic activity with the time-on-stream, although its initial activity was not as high as those of the other two catalysts. This result is closely related to the formation of nickel hydrosilicate. As evidenced from the TPR analysis listed in table 1, the $10Ni/SiO_2(873)$ catalyst showed the largest reduction peak for nickel hydrosilicate and also showed the best catalyst stability, as shown in table 3. Therefore, it can be concluded that the large Ni particles and the nickel hydrosilicate are responsible for enhancing the catalyst stability and, thus, leading to low catalyst deactivation.

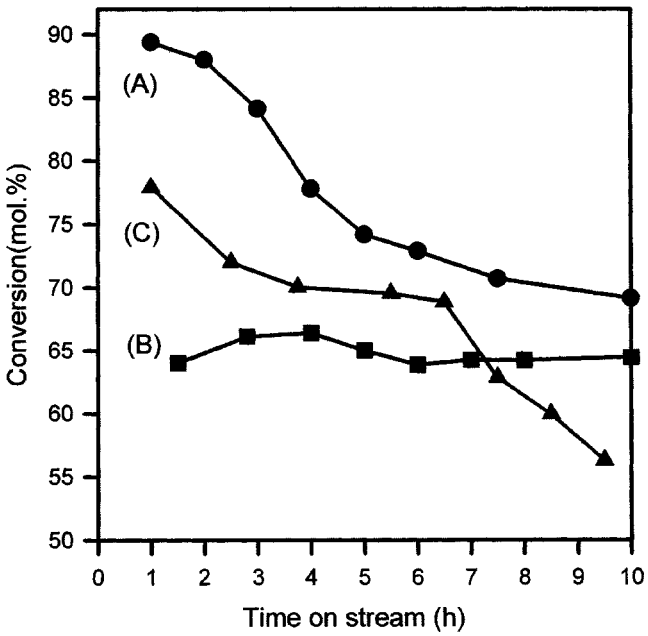

Figure 5. Effect of calcination temperature of $10Ni/SiO_2$ catalysts on the DCPA conversion at 573 K with time-on-stream (H_2/DCPA = 10): (A) $10Ni/SiO_2(723)$, (B) $10Ni/SiO_2(873)$ and (C) $10Ni/SiO_2(1073)$.

3.4. Catalysts deactivation

The deactivation of Ni/SiO_2 catalysts in the hydrodechlorination of DCPA can be explained in two ways. One is coke deposition [11,19] and the other one involves an interaction between metal and HCl [7,12,18]. In order to determine the effect of carbon deposit on catalyst deactivation, hydrodechlorination was carried out over Ni catalysts supported on a couple of acidic (γ-Al_2O_3, H-Y zeolite) and weakly acidic or non-acidic supports (SiO_2, TiO_2), which are summarized in table 5. Although coke deposition on the acidic supports was much higher than that on the weak or non-acidic supports, the Ni catalyst on the acidic supports showed a higher conversion of DCPA, suggesting that carbon deposition is not a major factor affecting catalyst deactivation. Therefore, our study focused on the possibility of Ni–HCl interaction.

A number of studies have been carried out to examine the effect of HCl on catalyst deactivation. Scott et al. [7] investigated the catalytic hydrogenolysis of 1,1,2-trichlorotrifluoroethane over palladium/zinc oxide catalysts supported on alumina. They reported that the suppression in hydrogenolysis activity was the result of the adsorption of

Table 5
Conversion of DCPA and coke deposition over Ni catalysts supported on various supports at 573 K after a 10 h run (H_2/DCPA = 10).

Catalyst	Conversion (%)	Dispersion (%)	Coke deposition (wt%)
10Ni/γ-Al_2O_3(723)	92.54	18.12	10.33
10Ni/H-Y zeolite (723)	76.11	19.67	15.71
10Ni/SiO_2(723)	69.14	9.06	2.43
10Ni/TiO_2(723)	63.38	18.66	1.08

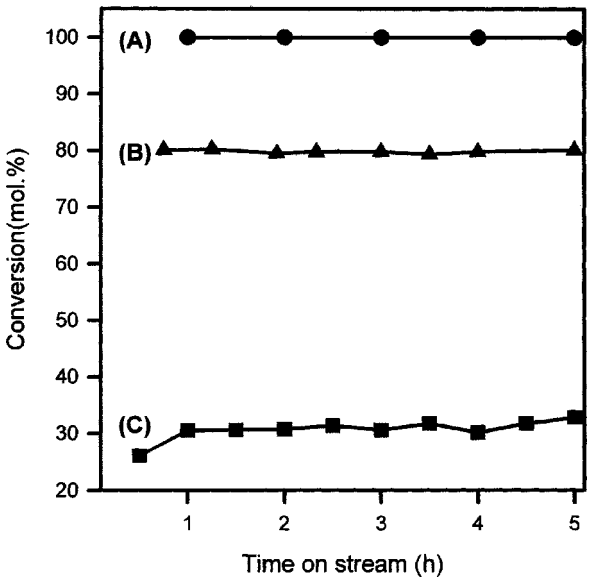

Figure 6. Catalytic activity of 10Ni/SiO_2(723) for the hydrogenation of propylene with time-on-stream at 573 K (H_2/propylene = 10): (A) freshly reduced, (B) regenerated by H_2 treatment for 2 h at 673 K after 10 h hydrodechlorination and (C) used for a 10 h period of hydrodechlorination.

Table 6
Conversion of propylene hydrogenation over fresh and used catalysts and regenerated catalysts after a 5 h run.[a]

Catalyst[b]	Conversion (%)	Dispersion (%)
A	100	9.06
B	32.85	7.03
C	80.09	8.75

[a] H_2/propylene = 10, reaction temperature 573 K.
[b] A fresh 10Ni/SiO_2(723) catalyst, B used 10Ni/SiO_2(723) catalyst after 10 h run, C used 10Ni/SiO_2(723) catalyst after 10 h run regenerated with hydrogen at 673 K for 2 h.

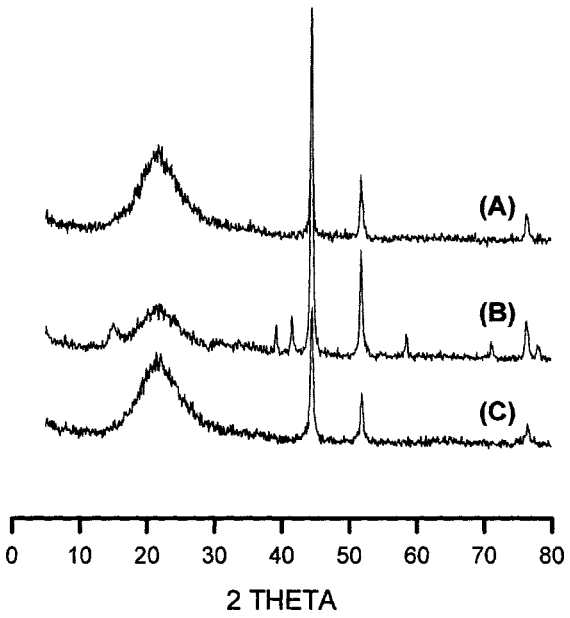

Figure 7. XRD patterns of 20Ni/SiO_2(723) catalysts: (A) freshly reduced, (B) used for a 10 h period of hydrodechlorination and (C) regenerated by H_2 at 673 K for 2 h after 10 h hydrodechlorination.

Cl on the metal. The adsorbed Cl reduced the metal surface area that was required for the dissociative chemisorption of hydrogen and, in addition, it changed the oxidation state of palladium from its initial metallic state to an oxidized state. Similar results were also reported by Shin et al. [18]. They suggested that the catalyst deactivation was due to an electronic effect between the adsorbed Cl and metal. The Cl, which was adsorbed on the nickel surface, depleted the d-orbital population of the surface nickel metal and changed the electronic structure of the active nickel component.

In order to confirm the influence of HCl on the deactivation of Ni/SiO_2 catalysts in the hydrodechlorination of DCPA, the hydrogenation of propylene was carried out over the fresh catalyst, the used catalyst, and the regenerated catalyst. After the hydrodechlorination of DCPA for a given time, the Ni/SiO_2 catalysts were treated with nitrogen for 2 h at 573 K. Propylene (2×10^{-3} mol/h) was then fed to the reactor for the hydrogenation, along with hydrogen (2×10^{-2} mol/h) and the helium carrier (3.8×10^{-2} mol/h). The feed ratio of hydrogen/propylene was 10. The reaction temperature was maintained at 573 K. Figure 6 shows data on propylene conversions over 10Ni/SiO_2(723) catalysts in different conditions. The fresh catalyst showed a 100% conversion to propane and no appreciable deactivation. On the other hand, the Ni/SiO_2 catalyst which was used for the hydrodechlorination of DCPA for 10 h, showed poor conversion, ca. 30%, although the conversion increased very slowly with the time-on-stream. This small enhancement in activity of the used catalyst is due to the regeneration of the deactivated Ni to metallic Ni by hydrogen. However, the activity of the Ni/SiO_2 catalyst, which had been regenerated by hydrogen at 673 K for 2 h after a 10 h hydrodechlorination, was recovered to 80% activity of the fresh catalyst. These results are related to the metal dispersion listed in table 6. As shown in table 6, the metal dispersion of the 10Ni/SiO_2(723) catalyst was decreased after reaction and the regenerated catalyst did not recover its initial metal dispersion. It was found from figure 6 and table 6 that the metal dispersion of catalysts was in good agreement with the propylene hydrogenation conversion for each catalyst. Therefore, it could be concluded that HCl deactivated Ni metal and it caused metal sintering.

In order to more precisely confirm the effect of regeneration, XRD measurements of freshly reduced, regenerated, and used Ni/SiO_2 catalysts were taken, as shown in fig-

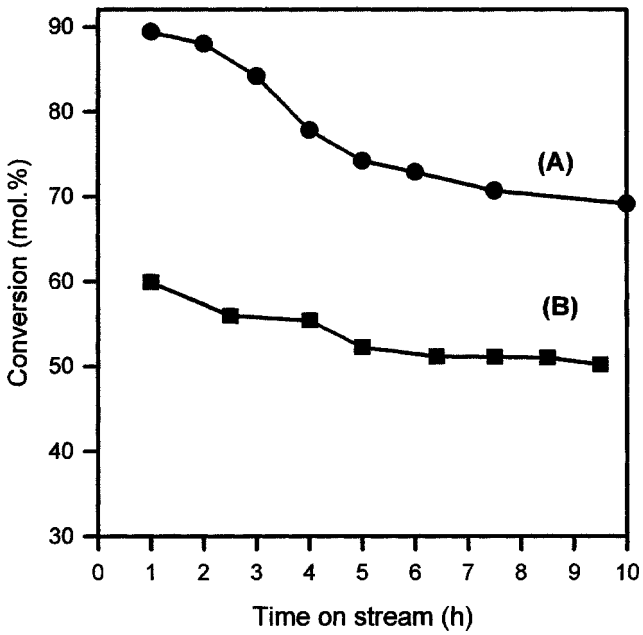

Figure 8. Comparison of catalytic activity of $10Ni/SiO_2(723)$ with time-on-stream at 573 K (H_2/DCPA = 10): (A) freshly reduced and (B) reduced by H_2 at 673 K for 2 h after a 2 h HCl pretreatment (3×10^{-2} mol/h) for freshly reduced catalyst.

ure 7. The used catalysts showed XRD patterns different from the fresh. XRD patterns of the fresh catalysts and the used catalysts with various Ni loadings were also represented in figures 3 and 4. However, the XRD patterns of the regenerated catalyst were nearly the same as those of the freshly reduced one. The above results indicate that the $NiCl_2$, formed due to Ni–HCl interaction, can be easily converted to Ni metal by hydrogen and that the hydrogenation activity of the Ni catalyst can be easily recovered by reduction with hydrogen. However, the hydrogenolysis activity of the Ni catalyst was not restored by reduction with hydrogen, as shown in figure 8. The Ni catalyst, which had been regenerated with hydrogen after a 2 h HCl pretreatment (3×10^{-2} mol/h) for freshly reduced catalyst, failed to recover its original activity, suggesting that the active sites of the nickel catalyst for hydrogenolysis were irreversibly deactivated as a result of the metal–HCl interaction [18].

4. Conclusions

The catalytic hydrodechlorination of 1,2-dichloropropane (DCPA) to propylene was carried out over Ni/SiO_2 catalysts in a continuous-flow fixed-bed reactor. The effects of Ni loading and calcination temperature on catalyst performance and catalyst deactivation were investigated. In the catalytic reaction, DCPA was selectively converted into propylene with a 95% or higher selectivity. The particle sizes of Ni on SiO_2 were well correlated with the catalyst stability. In terms of the effect of Ni loading, the $20Ni/SiO_2(723)$ catalyst showed the best stability in catalytic performance. TPR and UV-DRS measurements revealed that nickel hydrosilicate was formed as the result of the interaction between Ni and SiO_2. Nickel hydrosilicate was found to be responsible for the catalyst stability leading to low catalyst deactivation. It was also observed that HCl adsorption on the Ni/SiO_2 catalyst was the main source of catalyst deactivation. The adsorbed HCl modified the crystal structure of metallic Ni to $NiCl_2$ and led to irreversible catalyst deactivation and metal sintering.

References

[1] J. Stach, V. Pekarek, R. Endrst and J. Hetflejs, Chemosphere 39 (1999) 2391.
[2] N. Coute, J.D. Ortego, J.T. Richardson and M.V. Twigg, Appl. Catal. B 19 (1998) 175.
[3] D. Barrialt and M. Sylveste, Canad. J. Microbiol. 39 (1993) 594.
[4] M. Trillas, J. Peral and X. Domenech, J. Chem. Technol. Biotechnol. 67 (1996) 237.
[5] A. Gampine and D.P. Eyman, J. Catal. 179 (1998) 315.
[6] D.J. Moon, M.H. Chung, K.Y. Park and S.I. Hong, Appl. Catal. A 168 (1998) 159.
[7] S.P. Scott, T.J. Sweetman, A.G. Fitzgerald and E.J. Strurrock, J. Catal. 168 (1997) 501.
[8] B. Coq, J.M. Cognion, F. Figueras and D. Tournigant, J. Catal. 141 (1993) 21.
[9] B. Heinriches, P. Delhez, J. Schoebrechts and J. Pirard, J. Catal. 172 (1997) 322.
[10] A.D. Harley, T. Michael, D.D. Smith and M.D. Cisneros, US Patent 5 453 557.
[11] K.A. Frankel, B.W.-L. Jang, G.W. Roberts and J.J. Spivey, *Catalyst Deactivation* (1997) p. 239.
[12] B. Coq, G. Ferrat and F. Figueras, J. Catal. 101 (1986) 434.
[13] L.S. Vadlamannati, V.I. Kovalchuk and J.L. d'Itri, Catal. Lett. 58 (1999) 173.
[14] W. Ueda, S. Tomioka and Y. Morikawa, Chem. Lett. (1990) 879.
[15] T. Mori, W. Ueda and Y. Morikawa, Catal. Lett. 38 (1996) 73.
[16] J. van de Loosdrecht, A.M. van der Kraan, A.J. van Dillen and J.W. Geus, J. Catal. 170 (1997) 217.
[17] M.L. Jocomo, M. Schiavello and A. Cimino, J. Phys. Chem. 75 (1971) 1034.
[18] E.J. Shin and M.A. Keane, Appl. Catal. B 18 (1998) 241.
[19] H.C. Choi, S.H. Lee, O.B. Yang, J.S. Lee, K.H. Lee and Y.G. Kim, J. Catal. 161 (1996) 790.